Doi.org/10.36721/PJPS.2024.37.6.REG.1565-1580.1

Antioxidant activity of different polar parts of *Salix caprea* flower extract

Ruza Muhamet, Ke Zhang, Nuramina Mamat*, Meiheriguli Mijiti and Yongzhi Tian
Xinjiang Key Laboratory of Special Species Conservation and Regulatory Biology, College of Life Science,
Xinjiang Normal University, Urumqi, China

Abstract: This study evaluated the chemical composition and antioxidant activity of *Salix caprea* flower extract. The extract was divided into five different fractions using liquid-liquid extraction with petroleum ether (PEF), chloroform (CF), ethyl acetate (EAF), n-butanol (NF), and water (WR). The chemical constituents of the extracts were analyzed via gas chromatography-mass spectrometry. The quantification of total polyphenols and flavonoids was carried out using the Folin–Ciocalteu reagent and various colorimetric techniques. The antioxidant capacity of these fractions was tested by 2,2-Diphenyl-1-picrylhydrazyl (DPPH) free radical scavenging activity assay, 3-ethylbenzthiazoline-6-sulfonic acid radical cation ($ABTS^{+}$) scavenging activity assay and other methods. A total of 153 volatile substances were identified. The highest total polyphenol (40.02 mg/g) and flavonoid (78.62 mg/g) contents were in the EAF. EAF, NF and WR extracts demonstrates significant radical scavenging abilities against four types of free radicals, namely DPPH, ABTS, hydroxyl, and super oxide anion. Additionally, it exhibits strong reducing power towards Fe^{3+}.. These fractions improved cell viability, reduced malondialdehyde (MDA) and reactive oxygen species (ROS) levels, and increased catalase (CAT) and super oxide dismutase (SOD) activity in WRL-68 cells. The study highlights *Salix caprea* flower extract, particularly its n-butanol fraction, as a potential natural antioxidant source.

Keywords: *Salix caprea,* antioxidant, GC-MS, chemical composition, different polar parts, cell viability.

Submitted on 02-04-2024 – Revised on 13-08-2024 – Accepted on 23-08-2024

INTRODUCTION

Free radicals are characterized by unpaired electrons, making them highly reactive and unstable. These properties often initiate chain reactions, resulting in the oxidation of other molecules and the creation of additional free radicals or oxides (Jomova *et al*., 2023; He *et al*., 2019). Under normal physiological conditions, the generation and removal of reactive oxygen species (ROS) are balanced in a dynamic equilibrium, ensuring they remain harmless to the human body. However, the excessive production of oxygen free radicals disrupts the balance between the antioxidant defense system and oxygen free radicals (Yoshikawa and You., 2024). The buildup of reactive oxygen species (ROS) can cause oxidative stress, which in turn may lead to lipid peroxidation in cell membranes and the breakdown of proteins and enzymes and damage to nucleic acids, ultimately leading to various diseases, such as diabetes, aging, cardiovascular diseases and cancer (Feng and Wang, 2020; Hajam *et al*., 2022).

It has been indicated that antioxidants can help capture and neutralize free radicals, thus mitigating the effects of oxidative stress. Antioxidants can be categorized into two types: synthetic and natural. Synthetic antioxidants commonly used include compounds such as butylated hydroxyanisole (BHA), butylated hydroxytoluene (BHT), tertiary butylhydroquinone (TBHQ) and tertiary butyl catechol. (Chaudhary *et al*., 2024). However, synthetic antioxidants have been found to have harmful and carcinogenic effects on organisms (Li *et al*., 2023). Park *et al.* (Park *et al*., 2019) used astrocytes as a model to confirm that BHA may be potentially toxic to the nervous system, leading to brain and nerve development damage. On the other hand, natural antioxidants are highly favored due to their non-toxic side effects. In recent years, a large number of bioactive compounds with strong antioxidant activity have been identified in medicinal plants that are of high significance for the prevention of diseases, This includes conditions such as diabetes, atherosclerosis, hypertension, respiratory diseases, arthritis, cataracts, cancer and cardiovascular disorders (Nunes *et al*., 2016; Engwa *et al*., 2023).

Salix caprea is also known as mountain goat willow (fluffy willow, European fluffy willow, and big yellow willow) (Ahmed *et al*., 2017). It was found to exert antipyretic, analgesic, antibacterial, hemostatic, sedative and anthelmintic effects (Moohammadnor *et al*., 2010). The flavonoids in *Salix caprea* wood were also reported to have antifungal properties (Malterud *et al*., 1985). Astralgin, quercimeritrin and quercitin-3, 7-di-O-glucoside were identified in the pollen of Salix caprea (Gorobets *et al*., 1982). The leaves of Salix caprea were found to contain salicin, saligenin, gallocatechin, rutin, cynaroside, quercitin, and luteolin. *Previous research on Salix caprea has focused on its use as a feed additive to*

**Corresponding authors:* e-mails: Mynura@126.com

reduce ruminal methanogenesis in vitro (Bodas *et al*., 2009). In Unani medicine, a distillate made from the flowers of Salix caprea, known as Araq-e-Bedmusk, is commonly prescribed by Unani physicians. It is used to alleviate symptoms of nervousness and palpitation, as well as to support treatment for psychological stress and cardiac function abnormalities (Ahmed *et al*., 2017).

Regarding the existing research on Salix caprea, most studies have concentrated on its phytochemical composition, methods of cultivation, reproductive biology and geographical distribution (Ahmed *et al*., 2011; Terziolu *et al*., 2020). In general, the extraction methods significantly influence the chemical and functional properties of natural active ingredients, with solvents and other conditions playing a crucial role. To the best of our knowledge, studies on how different extraction solvents affect the functional activities and components of various parts of Salix caprea flower extracts are still limited. The chemical constituents and antioxidant activities of *Salix caprea* flowers extract from different polar parts were explored in this study.

MATERIALS AND METHODS

Materials and reagents

Salix caprea flower is purchased from Shenkang Biotechnology Co., Ltd. (Xinjiang, China), anhydrous ethanol, acetone, petroleum ether, chloroform, ethyl acetate, n-butanol, and methanol are all purchased from Beilian Fine Chemicals Development Co., Ltd. (Tianjin, China), all of them are all analytically pure. Gallic acid standard (SG8040), rutin standard (SR8250), BCA protein quantitative kit (P0010S) were obtained from Solebao (Beijing, China). Folinol reagents were manufactured by Yuanye Biotechnology Co., Ltd. (Shanghai, China S29851). 1-phenyl-2-picrylhydrazino radical (DPPH D807297) and 2-diazobis (3-ethylbenzothiazoline-6-sulfonic acid) diammonium salt ($ABTS^+$ A766844) were bought from McLean Biotechnology Co., Ltd. (Shanghai, China). Sodium carbonate (Na_2CO_3), sodium nitrite ($NaNO_2$), aluminum nitrate ($Al(NO_3)$), sodium hydroxide (NaOH), potassium persulfate ($K_2S_2O_8$), ferrous sulfate ($FeSO_4$), salicylic acid (SA), pyrogallol (PG), potassium ferricyanide ($K_3[Fe(CN)_6]$), trichloroacetic acid (TCA), ferric chloride ($FeCl_3$) and ascorbic acid (VC) were purchased from Zhiyuan Chemical Reagent Co., Ltd. (Tianjin, China). Tris-HCl from Blue season Biology (Shanghai, China). DMEM cell culture medium, mixture of trypsin, penicillin and streptomycin containing EDTA were manufactured from Gibco (Carlsbad, CA, USA). Fetal bovine serum (FBS) was obtained from Biological Industries (Kibbutz Beit Haemek, ISR). CCK-8 detection kit (E-CK-A362), superoxide dismutase (SOD E-BC-K019-M) detection kit, 3pyr4-methylenedioxyphenylpropionaldehyde (MDA E-BC-K028-M) detection kit, catalase (CAT E-BC-K031-M) kit and reactive oxygen species (ROS E-BC-K138-F) detection kit were all purchased from Ilerite Biotechnology Co., Ltd. (Wuhan, China). WRL-68 human normal hepatocytes were donated by Xinjiang University.

Preparation of extracts from the flowers of Salix caprea

To prepare the extracts from the flowers of *Salix caprea*, 500g of dried flowers were taken. After crushing, they were soaked in 70% ethanol (1:10) at room temperature. Then, the ultrasound-assisted extraction method was used to extract the flowers twice, with an interval of 72 hours between each extraction step. Finally, the two extracts were combined and the resulting extract was concentrated using a rotary evaporator (RE-3000A, Yarong biochemical instrument factory Shanghai, China) under reduced pressure to obtain the initial extract of *Salix caprea*. A small amount of distilled water was used to dissolve the extract, which was then poured into a separatory funnel. An equal amount of petroleum ether was added and the funnel was sealed and shaken. After standing still on a support stand for 12 hours, the petroleum ether extract layer of the *Salix caprea* extract was obtained. This extraction process was repeated two more times and the extracts were combined. The combined extract was then concentrated using a rotary evaporator under reduced pressure. After concentration, the liquid was freeze-dried in a freeze dryer for 48 hours. Finally, approximately 4.96 g of the petroleum ether extract layer of *Salix caprea* was obtained. Equal amount of chloroform, ethyl acetate, and n-butanol reagents were added sequentially and the same experimental steps were repeated to obtain the chloroform layer, ethyl acetate layer, n-butanol layer and water layer extracts of *Salix caprea*, which weighed approximately 2.05, 1.88, 14.32, and 79.00 g, respectively. The extraction rates were 0.992%, 0.41%, 0.376%, 2.864% and 15.8%, respectively.

GC-MS analyses

GC-MS analyses was established as previously described (Oyebode *et al*., 2020) with slight modification. Different extracts were obtained by removing Salix caprea flowers. The petroleum ether and chloroform fractions were dissolved in acetone, while the ethyl acetate, n-butanol, and water fractions were dissolved in methanol. The solution was then passed through a 0.22 μm micro porous membrane. The chromatographic column used is an HP-5msUI capillary column (Shimadzu, Kyoto, Japan) (30.0 m × 0.25 mm × 0.25 μm); the temperature program begins at 40°C, holding for 5 minutes, then increases at a rate of 10°C/min to 120°C, where it is held for 2 minutes. It then rises at a rate of 5°C/min to 160°C, held for another 5 minutes, followed by an increase at 5°C/min to 280°C, held for 5 minutes and finally increases at 5°C/min to 290°C, maintaining this temperature for 20 minutes. The injection port temperature is set at 290°C, with a split ratio of 10:1 and a column flow rate of 1.5 mL/min. For the MS conditions, the ion source temperature is set to

230°C, the transfer line temperature to 150°C, the auxiliary temperature to 300°C and the scanning range (m/z) is 35-400 Amu with a solvent delay of 3 minutes.

Measurement of total polyphenol and total flavonoid

The phenolic content was measured using a modified version of the Folin-Ciocalteu method, employing gallic acid as the standard (Yang *et al*., 2015). The sample was diluted to an appropriate multiple, then 200*u*L of the sample extract was taken and mixed with 5 mL of double distilled water and 1.5 mL of 5% Na_2CO_3. After avoiding light, 0.5 mL of Folin phenol reagent was added and the volume was made up to 10 mL. The reaction was carried out in a 75°C water bath for 10 minutes. After cooling, we used a microplate reader (Feyond-A300, ALLSHENG, Hangzhou, China) to measure the absorbance at 760 nm, and the phenolic content was determined using the calibration curve established with gallic acid, and the values were calculated accordingly, y = 0.0155x - 0.0019 and $R^2 = 0.9945$.

The total flavonoid content was assessed using the sodium nitrite-aluminum nitrate colorimetric assay, as described by Tang *et al.* (Tang *et al*., 2015).with a few modifications, 1 mL of the sample extract was taken and made up to 5 mL with 70% ethanol, then 0.3mL of 5% $NaNO_2$ was added. After 6 minutes of standing, 0.3mL of 10% $Al(NO)_3$ was added, followed by another 6 minutes of standing. Then, 4mL of 10% NaOH was added and made up to 10mL. After standing for 15 minutes, use a microplate reader (Feyond-A300, ALLSHENG, Hangzhou, China) to measure the absorbance at 760 nm, and the flavonoid content was determined using the equation of the calibration range established with rutin, i.e., y = 0.0013x + 0.005 and $R^2 = 0.9986$.

Determination of antioxidant activity in vitro

DPPH free radical scavenging ability

The DPPH radical scavenging activity was determined following the previously described method (Wu *et al*., 2003). Briefly, we took 1 mL of different concentrations of samples (0.2, 0.4, 0.6, 0.8 and 1mg/mL) and transferred them into test tubes. Further, we added 1mL of 0.15 mmol/L DPPH-ethanol solution to each tube, placed them in the dark for 20 minutes. Further, a microplate reader (Feyond-A300, ALLSHENG, Hangzhou, China) was employed to measure the absorbance A_1 at 517 nm. We used anhydrous ethanol instead of DPPH, and measure absorbance A_2 as a control group using the same method. In the blank control group, anhydrous ethanol was utilized instead of distilled water, and the absorbance A_0 was measured. We applied different concentrations of Vc solution as a positive control. Further, we calculated the scavenging rate of the samples for DPPH free radicals using the following equation:

$$\text{DPPH scavenging rate (\%)} = [1 - (A_1 - A_2)/A_0] \times 100\% \quad (1)$$

In this experiment,A_0 represents the absorbance of the control, while A_1 denotes the absorbance of the sample. Ascorbic acid was utilized as the positive control and a mixture of methanol and DPPH solution served as the negative control. Blanks consisted of methanol and extracts. The IC50 values were calculated to determine the concentration of the sample needed to scavenge 50% of DPPH free radicals.

$ABTS^+$ radical clear capability

The $ABTS^+$ radical scavenging activity was measured according to the method described by Wang *et al.* (Hou *et al*., 2011). We accurately measured 44.1 mg of $ABTS^+$ powder and dissolved it in 11.4823 mL of distilled water to prepare a 7 mM $ABTS^+$ solution. Then, we precisely weighed 11.31 mg of potassium persulfate powder and dissolved it in 298.85uL of distilled water to prepare a 140 mM potassium persulfate solution. After mixing 7.5 mL of 7 mM $ABTS^+$ solution with 132 uL of potassium persulfate solution and allowing it to react in the dark for 12 hours, a reaction occurred. Before the experiment, dilute with ethanol to create a working solution. The absorbance of the working solution at a wavelength of 734 nm should be 0.70±0.02. We transferred 1.0 mL of different sample concentrations (0.2, 0.4, 0.6, 0.8 and 1 mg/mL) in test tubes, added 1mL of $ABTS^+$ · determination solution to each of them and shook them for 10 seconds. Next, we let the samples stand for 6 minutes and used a microplate reader (Feyond-A300, ALLSHENG, Hangzhou, China) to measure A_1 at 734 nm. Ethanol without the sample while applying the same method to measure the absorbance A_2 served as the control group. We implemented different concentrations of Vc solution as the positive control. Then, we repeated the measurement three times and calculated the clearance rate (SC).

$$SC\ (\%) = (A_2 - A_1) / A_2 \times 100\%, \quad (2)$$

Hydroxyl radical scavenging capacity

The assay was determined following the method reported by Song *et al.* (Song *et al*., 2019) with minimal modifications. First, 1mL of samples with different concentrations (0.2, 0.4, 0.6, 0.8 and 1mg/mL) were transferred in graduated test tubes. Then, 1mL of 6.0 mmol/L ferrous sulfate solution and 1 mL of 6.0 mmol/L hydrogen peroxide solution were added to each tube, followed by vigorous shaking and letting the sample undisturbed for 10 minutes. Then, we added 1 mL of salicylic acid-ethanol solution, poured distilled water until the volume reached 10 mL. Further, after water-bathing at 37°C for 30 minutes, we used a microplate reader (Feyond-A300, ALLSHENG, Hangzhou, China) to measure the absorbance A_1 at 510 nm. Distilled water was used instead of hydrogen peroxide to measure the absorbance A_2 in the control group. Distilled water was utilized instead of the sample, and the absorbance A_0 was measured in the blank group using the same method. Different concentrations of Vc solution were used as

positive controls. The scavenging rate of hydroxyl radicals by the sample was calculated according to the following formula:

Inhibition rate (%) = [1 - (A_1 - A_2 / A_0] × 100% (3)

Superoxide anion radical scavenging activity

Hydroxyl radical scavenging assay was carried out using the method described by Li *et al.* (Li *et al*., 2008), and Shen *et al.* (Song *et al*., 2021), with some modifications. We took 1 mL of samples with different concentrations (0.2, 0.4, 0.6, 0.8 and 1 mg/mL), each into a graduated test tube. Then, we added 2.5 mL of 50 mmol/L Tris-HCl buffer solution and incubate at 25°C for 20 minutes. Cool to room temperature, add 1 mL of 3 mmol/L pyrogallol solution, dissolved in HCl solution (0.01 mol.L-1). We further mixed and incubated the specimens at 25°C water bath for 6 minutes. Finally, we added 0.1 mL of 8 mmol.L-1 HCl solution to stop the reaction, followed by measurements with a microplate reader (Feyond-A300, ALLSHENG, Hangzhou, China of the absorbance A_1 at 320 nm wavelength. We used distilled water instead of pyrogallol and measured the absorbance A_2 in the control group; Additionally, we utilized distilled water instead of the sample and measured the absorbance A_0 in the blank control group. Different concentrations of Vc solution were employed as positive controls. Finally, we calculated the superoxide anion clearance rate using the following formula:

Scavenging ability (%) = [1-(A_1-A_2)/A_0]× 100% (4)

Determination of reducing power

Reducing power was determined out according to the method described by Ahmadi *et al.* (Ahmadi *et al*., 2007). We took 1-mL samples of different concentrations (0.2, 0.4, 0.6, 0.8 and 1 mg/mL) and transferred them graduated test tubes and 2.5 mL of PBS (0.2 M, pH 6.6) To each sample, 2.5 mL of 1% potassium ferrocyanide solution was added. The mixtures were then incubated in a water bath at 50°C for 20 minutes. Subsequently, 2.5mL of 10% trichloroacetic acid solution was added. After centrifuging at 4000 rpm for 10 minutes, 2.5 mL of the supernatant was taken. To this, 2.5 mL of distilled water and 0.5 mL of 0.1% ferric chloride solution were added. The solutions were mixed thoroughly and left to stand for 10 minutes before measuring the absorbance at 700 nm (A_1).The absorbance A_0 was measured as a blank treatment using 1.0 mL of distilled water instead of the sample, following the same method. Different concentrations of Vc solution were used as positive controls. The reducing power of the samples was compared based on A_1-A_0, where a higher A_1-A_0 value indicates stronger reducing power of the sample.

Cell culture

Human normal hepatocyte WRL-68 was selected as the experimental platform. The cells were cultured in DMEM supplemented with 10% fetal bovine serum and 1% penicillin-streptomycin and cultured at 37°C in 5% CO_2 incubator (Panasonic Sanyo, Osaka, Japan).

Cell viability

Cellular viability was measured using the Cell counting kit-8 (CCK-8) (Feyond-A300, ALLSHENG, Hangzhou, China) assay.The cells were seeded in the log growth phase at a density of 2×10^5 cells/mL into a 96-well plate and incubated them for 24 hours. We then added different concentrations of the extract (6.25, 12.5, 25, 50, 100, 200, 400 and 800μmol/L) to the cells, with four replicates for each concentration and incubating in a CO_2 incubator (Panasonic Sanyo, Osaka, Japan), for 24 hours. 10 μL of CCK-8 reagent was added to each well, and incubating at 37^{o}C for 2 hours. Finally, we measured the absorbance at 450 nm using a microplate reader.

H_2O_2 induced model of oxidative damage in WRL-68 cells

H_2O_2 induced model was established as previously described (Gulcin, 2024) with slight modification. Cells in the exponential growth phase were seeded into 96-well plates at a concentration of 2×10^5 cells per mL and incubated for 24 hours. The cells were then exposed to varying concentrations of H_2O_2 (200, 300, 400, 500, 600, 700, 800, 900 and 1000μM) for 2 hours in a CO_2 incubator. Following this treatment, 100μL of serum-free medium containing 10μL of CCK-8 reagent (Feyond-A300, ALLSHENG, Hangzhou, China)was a dded to each well and incubated for an additional 2 hours at 37°C. Finally, the absorbance was measured at 450 nm using a microplate reader.

Protective effects of different polarity sites against H_2O_2-induced oxidative damage in WRL-68 cells

Cells in the logarithmic growth phase were seeded into 96-well plates at a density of 2×10^5 cells/mL and incubated for 24hours. Extracts from various polar regions were then added to the cells at concentrations of 6.25, 12.5, 25 and 50 μmol/L, followed by incubation in a CO_2 incubator for another 24 hours. After discarding the culture medium, the cells were washed three times with PBS. Next, a 500 μM H_2O_2 solution was added to each well, and the cells were incubated for 2 hours. This procedure was repeated four times for each concentration. Subsequently, 100 μL of serum-free medium containing 10 μL of CCK-8 reagent was added to each well, and the plates were incubated at 37°C for 2 hours. Finally, the absorbance at 450 nm was measured using a microplate reader.

Determination of the levels of SOD, MDA and CAT in the cells

The logarithmic growth phase cells were seeded at a density of 2×10^5 cells/mL in a 6-well plate and pre-treated with extract for 24 hours, followed by further incubation with 500 μM H_2O_2 for two hours. The cells were then

lysed and centrifuged (10,000×g, 4 minutes), and the supernatant was collected after washing with PBS. The levels of SOD, MDA and CAT in the supernatant were evaluated using assay kits.

Intracellular ROS levels determination

Cells (2×10^5 cells/mL) were cultivated in a 96-well plate, followed by incubation at 37°C for 24 hours. The cells were then treated with extract (24 hours) followed by H_2O_2 treatment (2 hours). The medium was removed and the cells were washed with PBS. Then, we added DCFH-DA dissolved in serum-free DMEM (100μL, 100μM) to each well and incubated the samples at 37°C for 30 minutes. Further, we washed them again with PBS. Finally, cells were cultured in 100μL serum-free DMEM, and fluorescence signals were detected using a fluorescence microplate reader (Feyond-A300, ALLSHENG, Hangzhou, China) at 37°C. The program settings were as follows: excitation wavelength at 485 nm, emission wavelength at 538 nm, measurement time of 30 minutes and readings at every 5 minutes. The results are expressed as the relative change in the fluorescence intensity (%).

STATISTICAL ANALYSIS

The data obtained in this study are presented as means ± standard deviations. The data were analyzed using GraphPad Prism, version 8.0 statistical software (GraphPad Software, San Diego, California, USA) through one-way ANOVA. Statistical significance was determined at $p<0.05$.

RESULTS

Chemical composition of VOCs in different polar parts of Salix caprea flowers extract

The ion flow diagrams of five different polar regions of the *Salix caprea* flowers extract were obtained (Appendix 1A–E). The GC-MS composition analysis results are presented in table 1. We identified a total number of 153 volatile substances, mainly belonging to eight categories, including esters, acids, alcohols, ketones, phenols, aldehydes, alkanes and alkenes. We identified 40, 55, 59, 77 and 42 components in the petroleum ether fraction, chloroform fraction, ethyl acetate fraction, n-butanol fraction, and water fraction, respectively.

Four components were found to be common among all fractions, namely n-hexadecanoic acid, 7-methyl-z-tetradecen-1-olacetate, 9,12,15-octadecatrienoic acid,2,3-dihydroxypropyl ester, (Z,Z,Z)- and ethyl iso-allocholate. Among them, the highest content of n-hexadecanoic acid was found in the chloroform and petroleum ether fractions, accounting for 91.16% in both fractions. The highest content in the ethyl acetate fraction was that of γ-sitosterol, accounting for 92.71%. The highest content in the water fraction was that of desulphosinigrin, accounting for 100%. The n-butanol fraction contained β-D-glucopyranose, 4-O-β-D-galactopyranosyl, and salicin, all with a percentage of 100%.

Table 1: The TPC and TFC of quinoa extracts.

Samples	TPC	TFC
PEF	9.91 ± 0.55	78.62 ± 1.99
CF	19.15 ± 1.65	70 ± 1.22
EAF	40.02 ± 2.66	68 ± 0.88
NF	25.28 ± 1.40	31.69 ± 1.26
WR	9.69 ± 0.86	41.08 ± 0.42

[1]TPC = total phenolic content (mg GAE/g); TFC = total flavonoid content (mg RE/g); PEF = petroleum ether fraction; CF = chloroform fraction; EAF = ethyl acetate fraction; NF = n-butanol fraction and WR = water residual.

Total phenolics and flavonoids content

Polyphenols are among the most abundant plant secondary metabolites, with flavonoids and phenolic acids being the two predominant types. These compounds are well-known for their excellent biological activities, including antioxidant and antidiabetic properties (Mcgivern *et al*.; Abubakar *et al*., 2014). The total phenolic content (TPC) and total flavonoid content (TFC) of the fractions are detailed in table 2. Among them, the ethyl acetate fraction (EAF) exhibited the highest levels, with TPC at 40.02 mg/g and TFC at 78.62 mg/g. This was followed by the n-butanol fraction (NF), the chloroform fraction (CF), the water residual (WR), and the petroleum ether fraction (PEF).

Antioxidant activity of different polar sites

The polar parts of *Salix caprea* flower extract showed certain DPPH radical scavenging ability, which was positively correlated with the mass concentration. At the same concentration, the order of clearance ability for DPPH is Vc> WR> EAF> NF> CF> PEF. When the concentration is 0.8mg/mL, WR, EAF and NF have a clearance rate of DPPH of over 91%. Among them, WR has a clearance ability equivalent to that of Vc at a concentration of 1mg/mL (fig. 1A).

The results of the clearance rate of $ABTS^+$ radicals by different polar parts of the *Salix caprea* flowers extract are shown in fig. 1B. Each part has the ability to clear $ABTS^+$ radicals. At a concentration of 0.6mg/mL, NF showed a slightly higher clearance rate of ABTS+ radicals (78.95%±0.27%) compared to Vc (78.65%±0.57%). At a concentration of 1 mg/mL, NF, WR and EAF showed a clearance rate of $ABTS^+$ radicals above 78.5% of Vc, with NF and WR achieving the same effect as Vc. This indicates that the *Salix caprea* flowers extract components NF, WR and EAR have strong activity in clearing $ABTS^+$ radicals (fig. 1B).

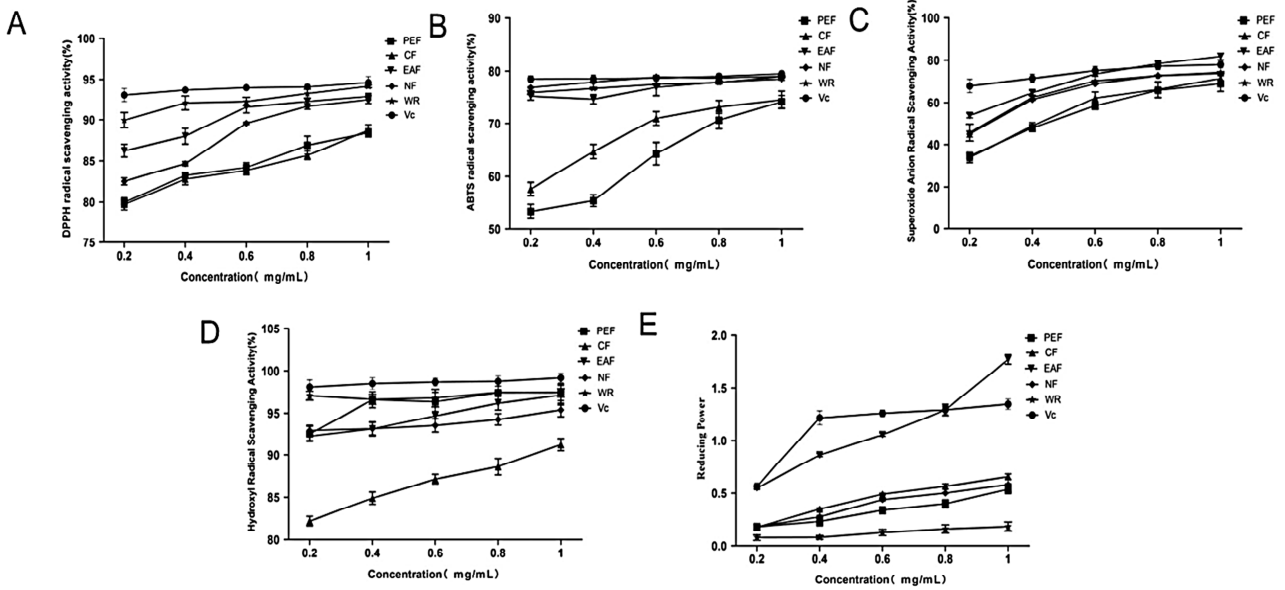

Fig. 1: The *in vitro* antioxidant activity of different polar parts. (A) The antioxidant activity of different polarity sites towards DPPH free radicals; (B) The antioxidant activity of different polarity sites towards $ABTS^{+}$ free radicals; (C) The antioxidant activity of different polarity sites towards hydroxyl radicals; (D) The antioxidant activity of different polarity sites towards super oxide anions; (E) The reducing power of different polarity sites ($P< 0.05$, n = 3).

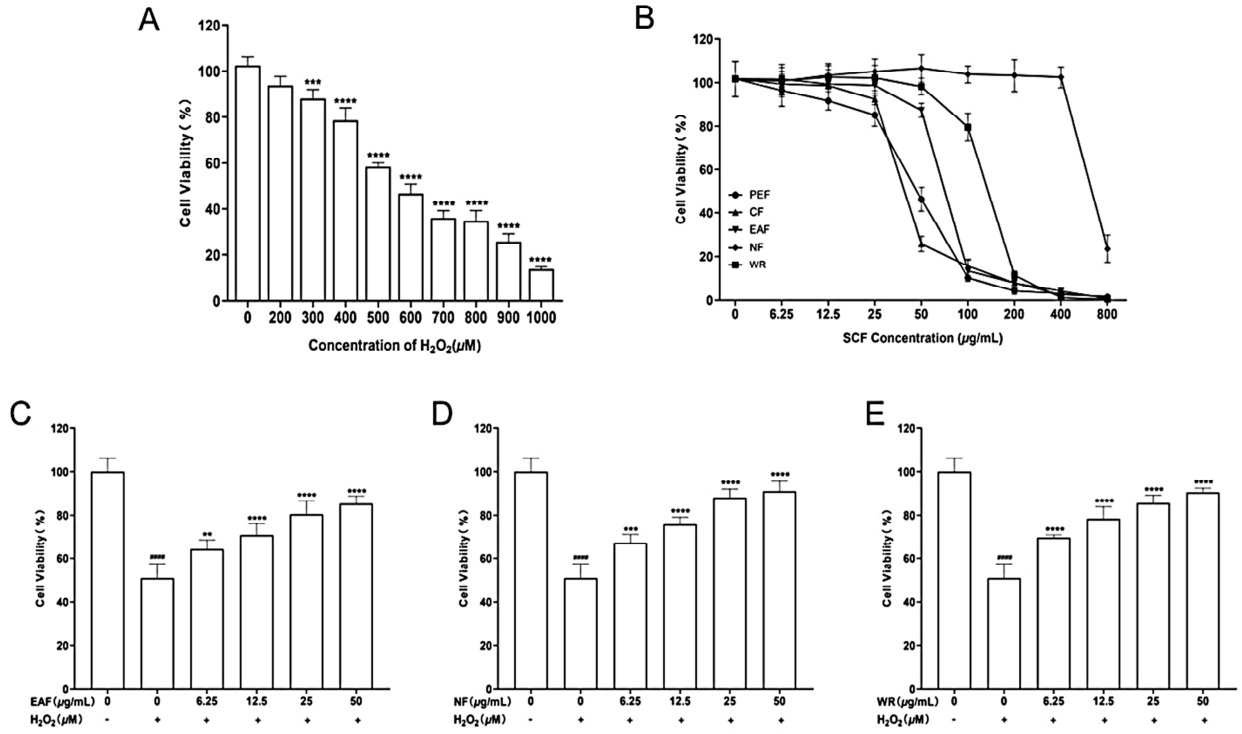

Fig. 2: (A) Impact of H_2O_2 on the viability of WRL-68 cells; (B) Impact of different polar parts of *Salix caprea* flowers extract on the viability of WRL-68 cells. (C) Protective effect of EAF site on WRL-68 cells; (D) Protective effect of NF site on WRL-68 cells; (E) Protective effect of WR site on WRL-68 cells. Significance: #### P<0.0001 vs. the control group.***P<0.001 and ****P<0.0001 vs. the control group. The data are expressed as mean ± SD (n = 5).

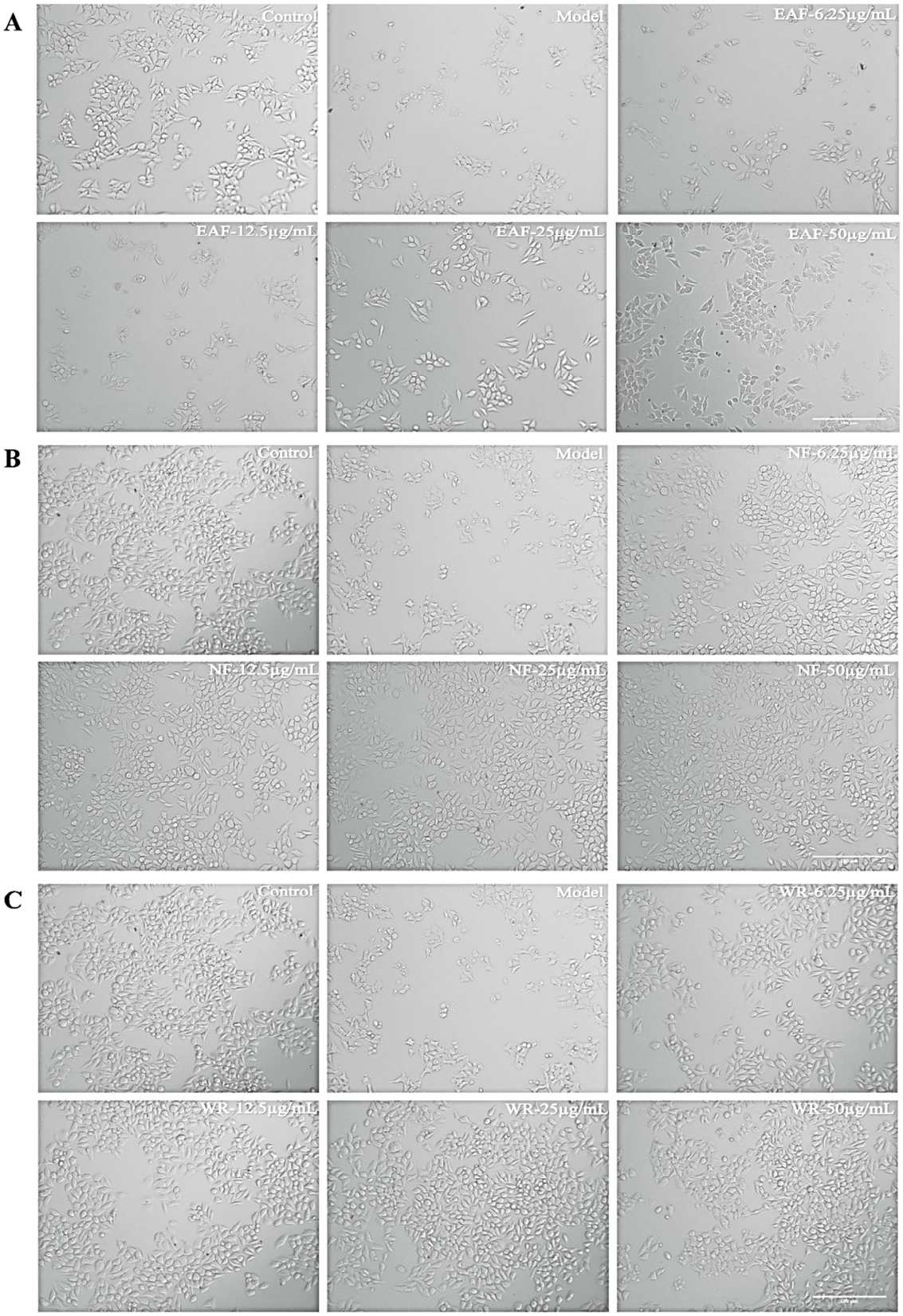

Fig. 3: Impact of different polarity locations on H_2O_2-induced WRL-68 cell morphology. (a) Effect of EAF on the cellular morphology of H_2O_2-induced WRL-68 (100×); (b) Effect of NF on the cellular morphology of H_2O_2-induced WRL-68 (100×); (c) Effect of WR on the cellular morphology of H_2O_2-induced WRL-68 (100×).

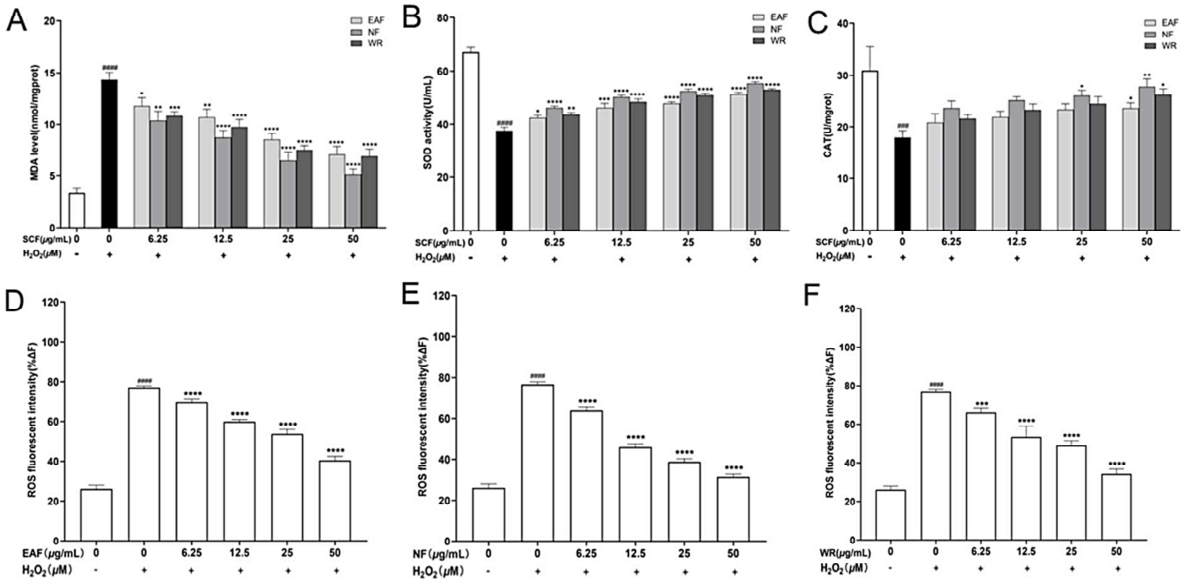

Fig. 4: (A-C) Effect of *Salix caprea* flowers extract from different polar parts on the levels of MDA, SOD, and CAT after H_2O_2-induced WRL-68 cell. (D) Effect of EAF on ROS levels of H_2O_2-induced WRL-68; (E) Effect of NF on ROS levels of H_2O_2-induced WRL-68;(F) Effect of WR on ROS levels of H_2O_2-induced WRL-68.damage. ### P<0.001 and #### P<0.0001 vs. the control group. *P<0.05, **P<0.01, ***P<0.001 and ****P<0.0001 vs. the H_2O_2-treated group. The data are expressed as mean ± SD (n = 4).

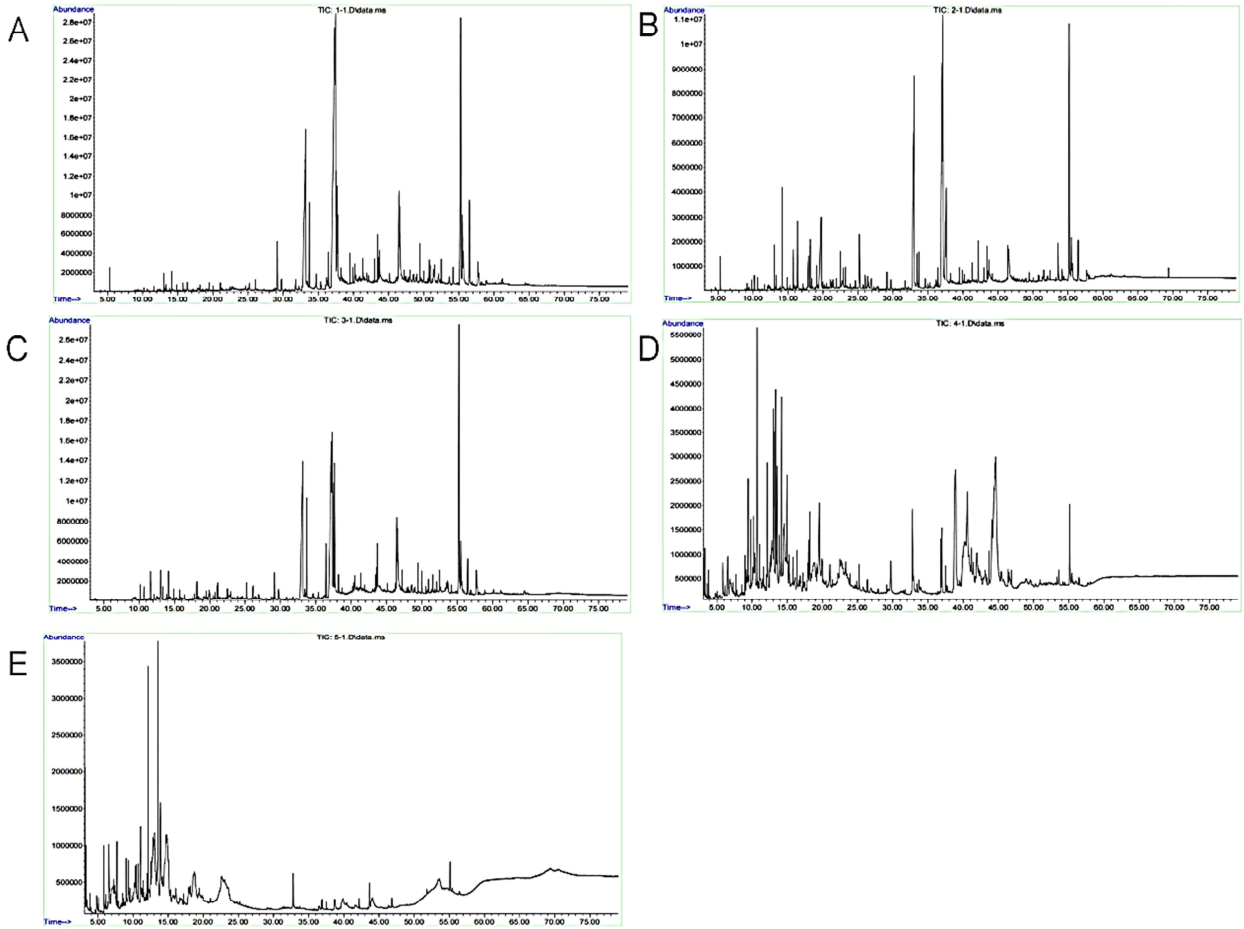

Appendix 1: Ion flow patterns in different polarity regions (A) Ion flow diagram of PEF; (B) Ion flow diagram of CF; (C) Ion flow diagram of EAF; (D) Ion flow diagram of WR; (e) Ion flow diagram of NF.

Table 2: *Salix caprea* flower extracts analyzed by GC-MS in different polar parts.

No	Classification	RT (min)	Chemical compounds	Area (%)				
				PEF	CF	EAF	NF	WR
1	Alcohols	10.177	Benzyl alcohol	—	1.29	1.52	—	—
2	Alcohols	10.672	1,2-cyclohexanediol	—	1.83	2.14	31.22	—
3	Alcohols	14.158	Salicyl alcohol	0.99	11.52	3.51	31.54	—
4	Alcohols	15.766	1,7-Octadien-3-ol, 2,6-dimethyl-	—	4.83	1.31	—	—
5	Alcohols	17.916	Heptan-2-ol,5-(2-tetrahydrofurfuryl)-	—	8.3	—	—	—
6	Alcohols	22.481	Phenol,4-(3-hydroxy-1-propenyl)-	—	5.65	2.16	—	—
7	Alcohols	25.208	4-((1E)-3-Hydroxy-1-propenyl)-2-methoxyphenol	—	12.65	3.83	5.72	—
8.	Alcohols	36.438	Phytol	2.87	3.68	9.71	—	—
9	Alcohols	43.435	Behenic alcohol	3.57	6.35	—	—	—
10	Alcohols	55.176	γ-Sitosterol	40.04	66.88	92.71	17.97	—
11	Alcohols	55.472	Cholest-5-en-3-ol,24-propylidene-,(3β)-	8.43	11.48	14.36	—	—
12	Alcohols	56.473	α-Amyrin	11.26	12.42	11.8	—	—
13	Alcohols	38.366	Ethanol,2-(9,12-octadecadienyloxy)-, (Z,Z)-	2.47	—	4.66	—	—
14	Alcohols	54.183	Stigmasterol	2.06	—	—	—	—
15	Alcohols	11.637	Phenylethyl Alcohol	—	—	2.65	—	—
16	Alcohols	15.774	1,7-Octadien-3-ol, 2,6-dimethyl	—	—	1.31	—	—
17	Alcohols	5.851	2-Furanmethanol	—	—	—	6.07	18.27
18	Alcohols	6.15	Benzeneethanol, α,β-dimethyl	—	—	—	1.73	4.92
19	Alcohols	7.036	(S)-(+)-2-Amino-3-methyl-1-butanol	—	—	—	9.07	36.64
20	Alcohols	8.547	2-Furanmethanol, 5-methyl	—	—	—	—	2.24
21	Alcohols	36.823	13-Heptadecyn-1-ol	—	—	—	—	2.22
22	Alcohols	3.603	2,3-Butanediol, [R-(R*,R*)]-	—	—	—	5.17	—
23	Alcohols	10.385	1,2,3,4-Butanetetrol, [S-(R*,R*)]-	—	—	—	12.79	—
24	Alcohols	13.023	Catechol	0.78	4.05	4.51	22.94	—
25	Phenols	18.407	Benzenemethanol,3-hydroxy-5-methoxy	—	1.39	—	—	—
26	Phenols	42.181	Phenol,2,2'-methylenebis[6-(1,1-dimethylethyl)-4-methyl	—	—	—	—	2.59
27	Phenols	15.846	2-Allylphenol	—	—	—	4.72	—
28	Aldehydes	13.117	Benzaldehyde,6-hydroxy-4-methoxy-2,3-dimethyl-	—	1.37	1.82	24.7	—
29	Aldehydes	23.235	Benzaldehyde,4-hydroxy-3,5-dimethoxy-	1.07	4.29	—	—	—
30	Aldehydes	13.118	Benzaldehyde,2-hydroxy-4-methoxy-3,6-dimethyl	—	—	1.82	24.7	—
31	Acids	14.889	Salicylic acid	—	1.99	1.8	26.82	—
32	Acids	19.109	Benzoic acid, 2-methoxy-1,6-Octadiene,3-ethoxy-3,7-dimethyl	—	3.72	—	—	—
33	Acids	20.539	Dodecanoic acid, 3-hydroxy-	0.65	2.32	2.29	—	5.91
34	Acids	27.878	Benzoic acid, 4-hydroxy-3,5-dimethoxy-	—	1.42	—	—	—
35	Acids	33.006	n-Hexadecanoic acid	54.79	91.16	89.28	18.08	12.74
36	Acids	36.181	Oleic Acid	4.88	2.25	1.71	—	—
37	Acids	37.166	9,12,15-Octadecatrienoic acid, (Z,Z,Z)-	26.21	71	44.24	—	—
38	Acids	38.268	1-Heptatriacotanol	—	1.36	—	23.92	—
39	Acids	41.315	Eicosanoic acid	6.81	4.36	—	—	—
40	Acids	26.087	Tetradecanoic acid	1.19	—	3.85	—	—
41	Acids	29.758	Pentadecanoic acid	1.32	—	—	—	—
42	Acids	32.233	9-Hexadecenoic acid	0.77	—	—	—	—

Continue...

43	Acids	35.347	Heptadecanoic acid	0.8	—	1.24	—	—	
44	Acids	13.902	Propanedioic acid,phenyl	—	—	1.13	—		
45	Acids	16.461	Dodecanoic acid,3-hydroxy	—	—	2.29	5.91	—	
46	Acids	19.94	Benzoic acid,4-hydroxy	—	—	3.21	—	—	
47	Acids	21.142	Benzoicacid,4-hydroxy-3-methoxy	—	—	3.8	—	—	
48	Acids	40.515	cis-5,8,11,14,17-Eicosapentaenoic acid	—	—	10.47	—	—	
49	Acids	47.198	cis-13-Eicosenoic acid	—	—	10.61	—	—	
50	Acids	3.31	Propanoic acid, 3-(acetylthio)-2-methyl-, (S)-	—	—	—	—	13.24	
51	Acids	6.662	o-Acetyl-L-serine	—	—	—	1.28	6.04	
52	Acids	7.287	Acetic acid, 2,2'-[oxybis(2,1-ethanediyloxy)]bis	—	—	—	4.82	14.56	
53	Ketones	5.291	2-Pentanone, 4-hydroxy-4-methyl	1.35	4.78	—	—	—	
54	Ketones	18.18	Acetophenone, 4'-hydroxy	—	7.94	—	—	—	
55	Ketones	22.92	2-Cyclohexen-1-one, 4-(3-hydroxy-1-butenyl)-3,5,5-trimethyl-, [R-[R*,R*-(E)]]-	—	4.39	—	—	—	
56	Ketones	24.642	(3-Oxo-2-pent-2-enylcyclopentyl)acetic acid	—	1.73	—	—	—	
57	Ketones	25.762	4-(1,5-Dihydroxy-2,6,6-trimethylcyclohex-2-enyl)but-3-en-2-one	—	1.6	1.86	—	—	
58	Ketones	29.145	2-Pentadecanone, 6,10,14-trimethyl-	4.72	4.29	6.03	—	—	
59	Ketones	57.847	Pregn-4-ene-3,20-dione,16,17-epoxy-, (16α)-	1.5	—	2.21	—	—	
60	Ketones	20.785	2-Butanone, 4-(4-hydroxyphenyl)-	—	—	1.43	—	—	
61	Ketones	22.923	3-Buten-2-ol,2-methyl-4-(1,3,3-trimethyl-7-oxabicyclo[4.1.0]hept-2-yl)-	—	—	2.25	—	—	
62	Ketones	7.723	1,2-Cyclopentanedione	—	—	—	3.83	9.58	
63	Ketones	9.029	2,4-Dihydroxy-2,5-dimethyl-3, (2H)-furan-3-one	—	—	—	4.74	7.87	
64	Ketones	10.712	2,5-Dimethyl-4-hydroxy-3(2H)-furanone	—	—	—	—	6.95	
65	Ketones	12.172	4H-Pyran-4-one, 2,3-dihydro-3,5-dihydroxy-6-methyl	—	—	—	15.26	50.67	
66	Ketones	4.823	D-Mannoheptulose	—	—	—	1.74	—	
67	Ketones	9.421	1,2-Cyclohexanedione	—	—	—	3.83	—	
68	Ketones	9.842	Cyclohexanone, 2-methyl-	—	—	—	9.24	—	
69	Ketones	11.509	Cyclopentane, 1-acetyl-1,2-epoxy-	—	—	—	3.83	—	
70	Ketones	5.256	Cyclohexanone, 2-(2-butynyl)-	—	—	—	5.8	—	
71	Ketones	21.068	2-(4-Nitrobutyryl)cyclooctanone	—	—	—	7.89	—	
72	Ketones	42.331	Androsta-1,4-dien-3-one, 17-hydroxy-17-methyl-, (17α)-	—	—	—	11.34	—	
73	Alkanes	39.496	Octadecane, 3-ethyl-5-(2-ethylbutyl)-	1.96	2.38	—	—	—	
74	Alkanes	58.054	Heptasiloxane,1,1,3,3,5,5,7,7,9,9,11,11,13,13-tetradecamethyl-	—	1.15	—	—	5.88	
75	Alkanes	59.989	Heptasiloxane, 1,1,3,3,5,5,7,7,9,9,11,11,13,13-tetradecamethyl-	—	—	—	—	5.88	
76	Alkanes	19.744	1,6-Octadiene, 3-ethoxy-3,7-dimethyl	0.91	41.61	—	—	—	
77	Alkanes	49.464	17-Pentatriacontene	3.29	—	5.3	—	—	
78	Alkanes	17.872	R-Limonene	—	—	3.55	9.51	—	
79	Esters	22.774	n-Butyric acid 2-ethylhexyl ester	—	3.03	12.44	—	—	
80	Esters	26.04	7-Methyl-Z-tetradecen-1-olacetate	9.88	11.88	11.29	56.57	12.2	
81	Esters	29.713	9-Octadecenoic acid, (2-phenyl-1,3-dioxolan-4-yl)methyl ester, trans-	—	2.33	3.36	11.09	—	
82	Esters	33.703	Hexadecanoic acid, ethyl ester	8.67	8.24	22.31	1.77	—	
83	Esters	37.499	Linoleic acid ethyl ester	—	11.88	—	—	—	
84	Esters	37.598	Octadecanoic acid	7.94	24.6	—	—	—	
85	Esters	39.926	Z-(13,14-Epoxy)tetradec-11-en-1-ol acetate	2.86	2.46	6.84	—	—	
86	Esters	43.686	Hexadecanoic acid, 1-(hydroxymethyl)-1,2-ethanediyl ester	—	8.74	4.77	—	—	
87	Esters	46.423	9,12-Octadecadienoic acid (Z,Z)-, 2,3-dihydroxypropyl ester	9.04	8.44	17.09	—	—	
88	Esters	46.535	9,12,15-Octadecatrienoic acid, 2,3-dihydroxypropyl ester, (Z,Z,Z)-	17.55	15.93	54.4	7.18	2.97	

Continue…

89	Esters	46.3	Ethyl iso-allocholate	19.62	10.69	46.58	4.09	15.34
90	Esters	43.71	Glycerol 1-palmitate	5.05	—	11.56	6.21	7.02
91	Esters	12.495	5-Amino-1-benzoyl-1H pyrazole-3,4-dicarbonitrile	—	—	1.42	—	—
92	Esters	19.999	Benzoic acid, 4-hydroxy-3-methoxy-, methyl ester	—	—	1.07	—	—
93	Esters	37.182	9,12-Octadecadienoic acid (Z,Z)-	—	—	90	9.67	—
94	Esters	37.521	9,12-Octadecadienoic acid, ethyl ester	—	—	22	—	—
95	Esters	3.185	Glycerin	—	—	—	3.14	24.73
96	Esters	3.24	Hydrazinecarboxylic acid,phenylmethyl ester	—	—	—	—	2.21
97	Esters	6.56	Propanoic acid, 3-nitro-, methyl ester	—	—	—	9.73	24.58
98	Esters	8.702	Imidazole,2-amino-5-[(2-carboxy)vinyl]	—	—	—	7.03	1.59
99	Esters	13.907	1,2,3-Propanetriol, 1-acetate	—	—	—	—	68.8
100	Esters	17.196	l-Gala-l-ido-octonic lactone	—	—	—	45.03	3
101	Esters	38.697	N,N'-Bis(Carbobenzyloxy)-lysine methyl(ester)	—	—	—	6.6	6.88
102	Esters	10.101	Diglycerol	—	—	—	9.36	—
103	Esters	17.432	12,15-Octadecadiynoic acid, methyl ester	—	—	—	2.32	—
104	Esters	18.212	3-Cyclohexene-1-methanol, α,α,4-trimethyl-, propanoate	—	—	—	16.42	—
105	Esters	20	4-Mercaptobenzoic acid, S methyl-, methyl ester	—	—	—	3.05	—
106	Esters	44.087	Limonen-6-ol, pivalate	—	—	—	32.09	—
107	Esters	37.662	9,12,15-Octadecatrienoic acid,ethyl ester, (Z,Z,Z)-	7.76	—	33.26	—	—
108	Other types	13.35	Benzofuran, 2,3-dihydro	—	1.75	1.78	—	—
109	Other types	16.353	2,7-Octadiene-1,6-diol, 2,6-dimethyl-	0.52	9.31	—	—	—
110	Other types	17.177	Furan-2-carbohydrazide,N2-(3-indolylmethylene)-	—	1.32	—	—	—
111	Other types	21.038	2-Oxabicyclo[3.3.0]oct-7-en-3-one,7-(1-hydroxypentyl)-	—	2.34	—	—	—
112	Other types	21.894	Tetrahydrofuran-2-one,5-[1-hydroxyhexyl]-	—	1.39	—	—	—
113	Other types	26.382	Benzoic acid, 4-hydroxy-3,5-dimethoxy-, hydrazide	—	2.77	—	2.31	—
114	Other types	26.905	2-Cyclohexen-1-one,4-hydroxy-3,5,5-trimethyl-4-(3-oxo-1-butenyl)-	—	3.81	—	—	—
115	Other types	33.43	1-Propyl-3,6-diazahomoadamantan-9-ol	—	8.32	—	1.88	—
116	Other types	53.59	6,7-Epoxypregn-4-ene-9,11,18-triol-3,20-dione,11,18-diacetate	0.66	8.37	—	4.8	—
117	Other types	25.185	9-Ethoxy-10-oxatricyclo[7.2.1.0(1,6)]dodecan-11-one	0.75	—	—	—	—
118	Other types	47.849	Z-5-Methyl-6-heneicosen-11-one	0.57	—	—	—	—
119	Other types	50.795	Octadecanal, 2-bromo	2.06	—	—	—	—
120	Other types	55.654	β-Amyrin	4.31	—	—	—	—
121	Other types	9.176	d-Glycero-d-ido-heptose	—	—	1.02	80	60.35
122	Other types	9.521	l-Gala-l-ido-octose	—	—	1.3	—	—
123	Other types	12.128	1,3-Benzodioxole,3a,7adihydro-2,2,4-trimethyl-	—	—	1.26	—	—
124	Other types	18.186	1-Oxaspiro[4.5]deca-3,6-diene,2,6,10,10-tetramethyl-	—	—	3.52	—	—
125	Other types	19.176	α-D-Glucopyranoside, O-α-D-glucopyranosyl-(1.fwdarw.3)-β-D_x005ffructofuranosyl	—	—	1.06	100	63.96
126	Other types	19.241	Guanosine	—	—	1.12	3.86	—
127	Other types	21.036	1,3-Cyclohexadiene-1-methanol, α,2,6,6-tetramethyl-, (.+-.)-	—	—	2.58	—	—
128	Other types	31.762	Estra-1,3,5(10)-trien-17β-ol	—	—	3.94	—	—
129	Other types	52.476	Ingol 12-acetate	—	—	4.79	—	—
130	Other types	4.822	β-D-Ribopyranoside, methyl	—	—	—	—	4.4
131	Other types	5.061	1H-Pyrazole-1-carbothioamide, 3,5-dimethyl-	—	—	—	1.36	4.14
132	Other types	11.093	Clindamycin	—	—	—	11.27	22.13
133	Other types	11.149	Methyl 6-oxoheptanoate	—	—	—	9.9	25.61
134	Other types	12.82	α-D-Galactopyranose, 2-(acetylamino)-2-deoxy	—	—	—	—	22.82

Continue...

135	Other types	13.55	Thiophene, 2-propyl-	—	—	—	21.58	90	
136	Other types	14.189	Desulphosinigrin	—	—	—	33.12	87.06	
137	Other types	14.703	L-Glucose	—	—	—	12.18	80	
138	Other types	16.101	β-D-Glucopyranose, 4-O-β-D-galactopyranosyl	—	—	—	100	14.04	
139	Other types	37.486	2-Myristynoyl pantetheine	—	—	—	—	1.93	
140	Other types	44.066	Paromomycin	—	—	—	28.45	17.39	
141	Other types	7.72	[1,3,4] Thiadiazol,2-amino-5-(2-piperidin-1-ylethyl)-	—	—	—	2.47	—	
142	Other types	9.189	Phenyl-β-D-glucoside	—	—	—	12.23	—	
143	Other types	10.189	3-O-Benzyl-d-glucose	—	—	—	14.47	—	
144	Other types	10.88	1-Hexanol, 4-methyl-, acetate	—	—	—	2.49	—	
145	Other types	12.566	Glucosamine, N-acetyl-Nbenzoyl	—	—	—	10.97	—	
146	Other types	13.363	Benzene, 1-ethynyl-4-fluoro	—	—	—	31.83	—	
147	Other types	14.483	D-Glucose, 6-O-α-D galactopyranosyl-	—	—	—	19.3	—	
148	Other types	14.601	5-KetoDfructose	—	—	—	34.41	—	
149	Other types	17.279	2H-Indeno[1,2-b]furan-2-one,3,3a,4,5,6,7,8,8b-octahydro-8,8-dimethyl	—	—	—	2.7	—	
150	Other types	18.051	2-Cyclohexylpiperidine	—	—	—	12.21	—	
151	Other types	19.944	3-Pyridinecarboxylic acid, 6-amino-	—	—	—	8.35	—	
152	Other types	38.889	Benzyl β-d-glucoside	—	—	—	90	—	
153	Other types	44.41	Salicin	—	—	—	100	—	

The results of the hydroxyl radical scavenging rate for different polarity fractions of the extract of *Salix caprea* flowers are illustrated in fig. 1C. With the increase in the sample concentration, the hydroxyl radical scavenging ability of each polarity fraction also gradually increases. At the same concentration, the order of scavenging ability is: Vc> PEF> WR> EAF> NF> CF. When the concentration is 1mg/mL, the hydroxyl radical scavenging rates of PEF, WR, EAF, and NF are (97.73%±0.41%), (97.41%±0.52%), (97%±1.14%) and (95.55%±0.72%), respectively, which is above 97% of Vc.

Fig. 1D displays the results of the clearance rate of superoxide anions by different polar parts of *Salix caprea* flowers extract. As the sample concentration increases, the clearance ability of each polar part towards superoxide anions gradually increases. At the same concentration, the clearance abilities are in following descending order: EAF > Vc> WR> NF> CF> PEF. At a concentration of 0.8 mg/mL, the clearance rate of superoxide anions by EAF (78.32%±0.28%) was higher than that of Vc (76.52%± 0.08%). When the concentration is 1mg/mL, the clearance rates of superoxide anions by WR, NF, CF and PEF were (74.21%±0.38%), (73.85%±0.14%), (71.39%±1.07%), and (70.32%±0.37%), respectively, which were all above 70.5% of Vc.

The results of the reduction ability of different polar parts of the *Salix caprea* flower extract are depicted in fig. 1E. All plant parts were found to have reduction ability and showed a clear dependence on sample concentration. The strength of reduction ability was found to be in the following order: EAF > Vc > CF > NF > PEF. However, WR had the poorest reduction ability, and the effect of its increase in the reduction ability with concentration was not significant. At a concentration of 1mg/mL, the reduction ability of EAF exceeded that of Vc, reaching 10 times that of WR.

Impact of Salix caprea flowers extract from different polar parts on the viability of WRL-68 cells

CCK-8 assay was performed to evaluate the toxicity of different polar parts of *Salix caprea* flowers extract on WRL-68 cells. As can be seen in fig. 2B, EAF showed no cytotoxicity and cell viability was close to 100% within the concentration range of 6.25-25μg/mL. However, toxicity was observed at concentrations between 50-800μg/mL. NF exhibited cell viability higher than 90% compared to the control group within the concentration range of 6.25-25μg/mL, with no apparent cytotoxicity, especially at concentrations between 12.5-400μg/mL, where the cell viability of NF was higher than 100%, indicating that NF can promote the growth of WRL-68 cells. At a concentration of 800μg/mL, the cell viability was only 23.54±6.33%. WR did not show cytotoxicity within the concentration range of 6.25-50μg/mL and at concentrations of 12.5 and 25μg/mL, it promoted cell

growth with a cell viability of 102.42±5.29%. Toxicity was observed starting from a concentration of 100μg/mL. Since both PEF and CF exhibited cytotoxicity within the concentration range of 6.25-800μg/mL, they were not selected for subsequent experiments. To save time, concentrations of 6.25μg/mL, 12.5, 25 and 50μg/mL were chosen for EAF, NF and WR in the subsequent experiments.

Protective effect of different polar parts of Salix caprea flowers extract on WRL-68 cells

H_2O_2 is a reactive oxygen species, an intermediate product in the human body's metabolism process. It easily penetrates the cell membrane and acts on some biomacromolecules, causing a series of reactions such as lipid per oxidation (Zhenxing *et al*., 2023). It is a common substance used to establish cell oxidative damage (Rebeiz *et al*., 2010). As can be observed in fig. 2A, with the increase of H_2O_2 concentration, the cell viability significantly decreases, indicating that the addition of H_2O_2 causes obvious damage to the cells. Thus, 500 μM was selected as the most appropriate modeling concentration for our subsequent experiments.

The effects of different polar parts of *Salix caprea* flowers extract on the cell survival rate of WRL-68 are shown in fig. 2C-E. Compared with the normal group, H_2O_2 treatment can lead to a decrease in cell activity. After pretreatment with the different polar parts of yellow willow flower extract, the number of viable cells increases in a concentration-dependent manner. Among them, the NF part has the best effect on the number of active cells. Compared with the normal group, the survival rate increased from (50.93±6.38)% in the H_2O_2 model group without NF to (67.26±3.93)%, (73.79± 1.79)%, (86±3.57)% and (90.98±3.76)%, respectively. The WR part comes next, with survival rates of (66.82± 3.48)%, (76.43±5.79)%, (85±3.7)% and (90.37±2.12)%, respectively. The ethyl acetate (EAF) part has the weakest effect, but still has a certain effect compared with the model group. The survival rate increases with concentration, reaching (64.19±4.48)%, (70.78±5.52)%, (80±6.05)% and (85.25±3.44)%, respectively.

In addition, the effects of EAF, NF and WR on the morphology of H_2O_2-induced WRL-68 cells are shown in fig. 3A-C. The cells in the normal group are spindle-shaped and very dense. But most of the model group WRL-68 cells are close to round and the cell density is lower than normal, indicating apoptosis. After pretreatment with different polar parts, the cell morphology returns to normal. These experiments indicate that different polar parts of *Salix caprea* flowers extract have a certain protective effect on the oxidative stress-induced damage to WRL-68 cells. These findings suggest that.

Effect of Salix caprea flowers extract from different polar parts on the levels of MDA, SOD and CAT after H_2O_2-induced WRL-68 cell damage

According to fig. 4A-C, compared with the normal group, the MDA content in the model group showed a significant increase (P<0.0001) and the activities of other enzymes showed a significant decrease (P<0.0001), indicating a successful model of cell oxidative damage after H_2O_2 treatment. Compared with the model group, the pretreatment with different polar parts significantly reduced the cellular MDA content (P<0.05, P<0.01, P<0.001, P<0.0001), significantly increased the cellular SOD and CAT activities (P<0.05, P<0.01, P<0.001, P<0.0001) and showed concentration dependence. Each sample group made the various indicators tend toward the level of the normal group cells, indicating that the different polar parts of *Salix caprea* flowers extract exerted a pre-protective effect on WRL-68 cell oxidative damage by changing the cellular MDA, SOD, and CAT levels.

Effects of Salix caprea flowers extract from different polar positions on the intracellular ROS levels induced by H_2O_2 in WRL-68 cells

As shown in fig. 4C-F, after WRL-68 cells were treated with H_2O_2, the intracellular ROS levels increased threefold compared to the control group (P<0.0001). However, when the extracts from four different parts (6.25, 12.5, 25 and 50μg/mL) were utilized for intervention, the ROS levels significantly decreased compared to the model group, with significant differences (P<0.001, P<0.0001).

DISCUSSION

In this experiment, we employed liquid-liquid extraction combined with GC-MS technology to analyze the chemical compositions of different polarity parts of *Salix caprea* flowers extract. A number of 153 volatile substances were identified, mainly belonging to eight categories, including esters, acids, alcohols, ketones, phenols, aldehydes, alkanes, and alkenes. Among them, n-hexadecanoic acid had the highest content in the chloroform and petroleum ether fractions, accounting for 91.16% in both fractions. The highest content in the ethyl acetate fraction was γ-sitosterol, accounting for 92.71%. The highest content in the water fraction was desulphosinigrin, accounting for 100%. The n-butanol fraction contained β-D-glucopyranose, 4-O-β-D-galactopyranosyl and salicin, all with a percentage of 100%. Song *et al.* (Ganesan *et al*., 2022) determined the antioxidant activity of n-hexadecanoic acid from the leaves of *Ipomoea eriocarpa*. The study found that n-hexadecanoic acid had significant antioxidant activity, capable of scavenging free radicals, possessing certain reducing power, chelating iron ions, and demonstrating overall antioxidant activity. Additionally, n-hexadecanoic

acid also exerted protective effects on cells, alleviating oxidative damage. Nisha *et al.* (RAKESH *et al*., 2013). adopted GC-MS technique to isolate and identify γ-sitosterol from the roots of *Girardinia heterophylia*. Yousef *et al.* (Al-Saraireh *et al*., 2020), analyzed the chemical composition of *Euphorbia hierosolymitana* Boiss. crude extract by GC-MS technology, and desulphosinigrin was found in n-butanol part and ethyl acetate part and the content was 0.51% and 4.38%, respectively. Harish *et al.* (Kommera *et al*., 2010) discovered a significant toxic effect on cancer cells and the ability to inhibit cancer cell growth and survival through the synthesis of β-D-glucopyranose. Al *et al.* (Al Bujuq *et al*., 2017) chemically synthesized 4-O-β-D-galactopyranosyl and evaluated its cytotoxicity. It showed high anticancer activity and was able to inhibit the growth and survival of cancer cells, thus having potential as a candidate compound for anticancer drugs. Guo *et al.* (Guo *et al*., 2019) found that salicin prevented TNF-A-induced aging of human umbilical vein endothelial cells (HUVECs). These findings suggest that salicylate may have anti-aging potential.

Herein, the antioxidant capacities of five different polarity parts of *Salix caprea* flowers extract are mainly studied by *in vitro* chemical methods. In DPPH, ABTS, superoxide anion radical, hydroxyl radical four free radical scavenging models and reducing power model, the results show that the extracts of each part have good *in vitro* antioxidant capacity. Among them, the EAF part has the best antioxidant activity, followed by NF and WR, PEF part and CF part gradually weaken, indicating that the types and structures of the main antioxidant active components contained in different polarity parts of yellow flower willow extract may be related. Therefore, in different antioxidant systems, the antioxidant effects of different polarity parts of *Salix caprea* flowers extract are different. In the body, reactive oxygen species (ROS) include superoxide anion radicals, hydroxyl radicals, and non-radical species like hydrogen peroxide. These ROS not only cause oxidative damage in humans but also contribute to food spoilage (Aruoma *et al*., 1991). Therefore, using natural antioxidants can effectively alleviate oxidative stress in the human body and certain diseases.

In this study, the total phenols and total flavonoid contents of different parts were determined. The ethyl acetate fraction (EAF) showed the highest TPC (40.02 mg/g) and TFC (78.62mg/g), followed by n-butanol fraction (NF), chloroform fraction (CF), water residual (WR), and petroleum ether fraction (PEF).

The protective effect of different polar parts on H_2O_2-induced oxidative stress in WRL-68 cells is evaluated (Wu *et al*., 2017). Pre-treating WRL-68 cells with EAF, NF, and WR fractions can significantly elevate the decrease of SOD and CAT induced by H_2O_2, which can significantly reduce the increase of MDA and ROS induced by H_2O_2 and have a protective effect on H_2O_2-induced WRL-68 cell damage. These results provide experimental basis for the future study and development of the antioxidant mechanism of *Salix caprea* flowers extract EAF, NF and WR fractions.

The antioxidant system, which includes both antioxidants and antioxidative enzymes, plays a crucial role in regulating the balance between oxidation and reduction processes (He *et al*., 2022; Li *et al*., 2022; Zhang *et al*., 2022). As reported, enzymes such as superoxide dismutase (SOD) and catalase (CAT) serve as the primary defense mechanism against reactive oxygen species (ROS), effectively scavenging free radicals likeO_2^- and HO^-(Liang *et al*., 2018; Tsai *et al*., 2020). Superoxide dismutase (SOD) catalyzes the conversion of superoxide anion (O_2^-) into hydrogen peroxide (H_2O_2). Subsequently, catalase (CAT) breaks down the hydrogen peroxide into water (H_2O) and oxygen (O_2). Excessive oxidative stress can lead to elevated levels of MDA and ROS (Li *et al*., 2023a). In this study, it was found that pretreating WRL-68 cells with different polar parts of *Salix caprea* flowers extract significantly elevated the H_2O_2-induced SOD and CAT levels, while significantly reducing the H_2O_2-induced MDA and ROS levels.

CONCLUSION

This study highlights the significant antioxidant potential of various polar fractions of *Salix caprea* flower extract. The ethyl acetate (EAF), n-butanol (NF) and water (WR) fractions exhibited the strongest antioxidant activities, demonstrating their capacity to scavenge free radicals, reduce oxidative stress markers and enhance the viability of WRL-68 cells. These findings underscore the potential of *Salix caprea* flower extract, particularly the n-butanol fraction, as a promising natural source of antioxidants. This could have valuable implications for the development of natural antioxidant therapies aimed at mitigating oxidative stress-related conditions. Further research is recommended to explore the specific bioactive compounds responsible for these effects and their mechanisms of action.

ACKNOWLEDGEMENTS

The authors would like to express their gratitude to the Xinjiang Key Laboratory of Special Species Conservation and Regulatory Biology at Xinjiang Normal University for providing the facilities to conduct this research. This work was supported by the Xinjiang Autonomous Region University Research Project (XJEDU2023P076) and the Xinjiang Normal University PhD Start-up Fund (XJNUBS2205).

REFERENCES

Abubakar MB, Abdullah WZ, Sulaiman SA and Ang BS (2014). Polyphenols as key players for the antileukaemic effects of propolis. *Evid-Based Compl. Alt.*, 371730.

Ahmadi F, Kadivar M and Shahedi M (2007). Antioxidant activity of Kelussia odoratissima Mozaff. in model and food systems. *Food Chem.,* **105**(1): 57-64.

Ahmed A, Akbar S and Shah WA (2017). Chemical composition and pharmacological potential of aromatic water from *Salix caprea* inflorescence. *Chin. J. Integr. Med.,* pp.1-5.

Ahmed A, Shah WA, Akbar S, Younis M and Kumar D (2011). A short chemical review on *Salix caprea* commonly known as goat willow. *Int. J. Res. Phytochem. Pharmacol.,* **1**(1): 17-20.

Al-Saraireh YM, Youssef AMM, Alsarayreh AZA, Hujran TAA and Garrido G (2020). Phytochemical and anti-cancer properties of Euphorbia hierosolymitana Boiss. crude extracts. *J. Pharm. Pharmacogn. R.*, **9**(1): 13-23.

Al Bujuq N, Arar S and Khalil R (2018). Synthesis and cytotoxic activity of 4-O-β-D-galactopyranosyl derivatives of phenolic acids esters. *Nat. Prod. Res.,* **32**(22): 2663-2669.

Aruoma OI, Kaur H and Halliwell B (1991). Oxygen free radicals and human diseases. *J. Epidemiol. Commun. H.*, **111**(5): 172-177.

Bodas R, Lopez S, Fernández M, García-González R, Wallace RJ and González JS (2009). Phytogenic additives to decrease *in vitro* ruminal methanogenesis. *Options Mediterranéenn*es, **85**: 279-283.

Chaudhary P, Janmeda P, Setzer WN, Aldahish AA, Sharifi-Rad J and Calina D (2024). Breaking free from free radicals: Harnessing the power of natural antioxidants for health and disease prevention. *Chem. Pap.,* **78**(4): 2061-2077.

Engwa GA, Nweke FN and Nkeh-Chungag BN (2022). Free radicals, oxidative stress-related diseases and antioxidant supplementation. *Altern. Ther. Health M.*, **28**(1): 114-128.

Feng T and Wang J (2020). Oxidative stress tolerance and antioxidant capacity of lactic acid bacteria as probiotic: A systematic review. *Gut Microbes,* **12**(1): 1801944.

Ganesan T, Subban M, Christopher Leslee DB, Kuppannan SB and Seedevi P (2024). Structural characterization of n-hexadecanoic acid from the leaves of Ipomoea eriocarpa and its antioxidant and antibacterial activities. *Biomass Convers. Biorefin*., **14**: 14547-14558.

Gorobets AV, Bandyukova VA and Shapiro DK (1982). Flavonoid composition of the pollen (pollen pellets) from *Salix caprea* and *S. alba. Chem. Nat. Compd.,* **18**(6): 747-748.

Gulcin I (2020). Antioxidants and antioxidant methods: An updated overview. *Arch Toxicol.,* **94**(3): 651-715.

Guo F, Wu R and Xu J (2019). Salicin prevents TNF-α-induced cellular senescence in human umbilical vein endothelial cells (HUVECs). *Artificial Cells*, **47**(1): 2618-2623.

Hajam YA, Rani R, Ganie SY, Sheikh TA, Javaid D, Qadri SS, Pramodh S, Alsulimani A, Alkhanani MF, Harakeh S, Hussain A, Haque S and Reshi MS (2022). Oxidative stress in human pathology and aging: Molecular mechanisms and perspectives. *Cells*, **11**(3): 552.

He C, Gao M, Zhang X, Lei P, Yang H, Qing Y and Zhang L (2022). The protective effect of sulforaphane on Dextran sulfate sodium-induced colitis depends on gut microbial and Nrf2-related mechanism. *Front. Nutr.*, **9**: 893344.

He Y, Bu LJ, Xie HD and Liang GZ (2019). Antioxidant activities and protective effects of duck embryo peptides against HO-induced oxidative damage in HepG2 cells. *Poult. Sci.,* **98**(12): 7118-7128.

Hou DX, Korenori Y, Tanigawa S, Yamada-Kato T, Nagai M, He X and He J (2011). Dynamics of Nrf2 and Keap1 in ARE-mediated NQO1 expression by Wasabi 6-(Methylsulfinyl)hexyl isothiocyanate. *J. Agric. Food Chem.*, **59**(22): 11975-11982.

Jomova K, Raptova R, Alomar SY, Alwasel SH, Nepovimova E, Kuca K and Valko M (2023). Reactive oxygen species, toxicity, oxidative stress and antioxidants: Chronic diseases and aging. *Arch. Toxicol.*, **97**(10): 2499-2574.

Kommera H, Kaluđerović GN, Bette M, Kalbitz J, Fuchs P, Fulda S, Mier W and Paschke R (2010). *In vitro* anticancer studies of alpha- and beta-D-glucopyranose betulin anomers. *Chem. Biol. Interact.*, **185**(2): 128-136.

Li H, Yang TX Zhao QS and Zhao B (2023). Protective effect of cannabidiol on hydrogen peroxide-induced oxidative damage in human umbilical vein endothelial cells (HUVECs). *Chem. Biodivers*, **20**(7): e202300169.

Li N, Wen L, Wang F, Li T, Zheng H, Wang T and Li M (2022). Alleviating effects of pea peptide on oxidative stress injury induced by lead in PC12 cells via Keap1/Nrf2/TXNIP signaling pathway. *Front. Nutr,* **9**: 964938.

Li S, Xie J, Bai Y, Jiang Z, Li K and Wu C (2023). Synthetic phenolic antioxidants evoked hepatoxicity in grass carp (*Ctenopharyngodon idella*) through modulating the ROS-PI3K/mTOR/AKT pathway: Apoptosis-autophagy crosstalk. *Fish Shellfish Immun.*, **139**: 108906.

Li Y, Jiang B, Zhang T, Mu W and Liu J (2008). Antioxidant and free radical-scavenging activities of chickpea protein hydrolysate (CPH). *Food Chem.*, **106**(2): 444-450.

Liang M, Wang Z, Li H, Cai L, Pan J, He H, Wu Q, Tang Y, Ma J and Yang L (2018). L-Arginine induces antioxidant response to prevent oxidative stress via

stimulation of glutathione synthesis and activation of Nrf2 pathway. *Food Chem. Toxicol.*, **115**: 315-328.

Liang Z, Yang Y, Wu X, Lu C, Zhao H, Chen K, Zhao A, Li X and Xu J (2023). GAS6/Axl is associated with AMPK activation and attenuates H_2O_2-induced oxidative stress. *Apoptosis*, **28**(3): 485-497.

Malterud KE, Bremnes TE, Faegri A, Moe T, Dugstad EKS, Anthonsen T and Henriksen LM (1985). flavonoids from the wood of *Salix caprea* as inhibitors of wood-destroying fungi. *J. Nat. Prod.*, **48**(4): 559-563.

McGivern BB, Tfaily MM, Borton MA, Kosina SM, Daly RA, Nicora CD and Wrighton KC (2021). Decrypting bacterial polyphenol metabolism in an anoxic wetland soil. *Nat. Commun.*, **12**(1): 2466.

Moohammadnor M, Tursun X, Ling QM, Sultan A and Eshbakova KA (2010). Flavonoids from *Salix caprea*. *Chem. Nat. Compd.,* **46**: 799-800.

Nunes JC, Lago MG, Castelo-Branco VN, Oliveira FR, Torres AG, Perrone D and Monteiro M (2016). Effect of drying method on volatile compounds, phenolic profile and antioxidant capacity of guava powders. *Food Chem.*, **197**(APR.15PT.A): 881-890.

Oyebode O, Erukainure OL, Zuma L, Ibeji CU, Koorbanally NA and Islam MS (2022). *In vitro* and computational studies of the antioxidant and anti-diabetic properties of *Bridelia ferruginea. J. Biomol. Struct. Dyn.*, **40**(9): 3989-4003.

Park S, Lee JY, Lim W, You S and Song G (2019). Butylated hydroxyanisole exerts neurotoxic effects by promoting cytosolic calcium accumulation and endoplasmic reticulum stress in astrocytes. *J. Agric. Food Chem.,* 67(34): 9618-9629.

Rakesh, Singh, Nishatripathi, Sunita and Kumar (2013). Isolation and identification of γ-sitosterol by GC-MS from roots of *Girardinia heterophylia. Orient J. Chem.*, **29**(2): 705-707.

Rebeiz CA, Benning C, Bohnert HJ, Daniell H, Hoober JK, Lichtenthaler HK and Tripathy BC (Eds.) (2010). The chloroplast: Basics and applications. Springer Science & Business Media, **31**: 106-130.

Song Q, Jiang L, Yang X, Huang L, Yu Y, Yu Q, Chen Y and Xie J (2019). Physicochemical and functional properties of a water-soluble polysaccharide extracted from Mung bean (*Vigna radiate* L.) and its antioxidant activity. *Int. J. Biol. Macromol.*, **138**: 874-880.

Song S, Liu X, Zhao B, Abubaker M, Huang Y and Zhang J (2021). Effects of *Lactobacillus plantarum* fermentation on the chemical structure and antioxidant activity of polysaccharides from bulbs of Lanzhou lily. *ACS Omega*, **6**(44): 29839-29851.

Tang Y, Li X, Zhang B, Chen PX, Liu R and Tsao R (2015). Characterisation of phenolics, betanins and antioxidant activities in seeds of three *Chenopodium quinoa* Willd. genotypes. *Food Chem.,* **166**(1): 380-388.

Terziolu S, Serdar B, Cokunelebi K and Zturk M (2020). Reporting intersex florets in *Salix caprea* L. (Salicaceae) from NE Anatolia. *Kastamonu Univ. J. For.*, **20**(1): 11-14.

Tsai BC, Hsieh DJ, Lin WT, Tamilselvi S, Day CH, Ho TJ, Chang RL, Viswanadha VP, Kuo CH, Huang CY. (2020). Functional potato bioactive peptide intensifies Nrf2-dependent antioxidant defense against renal damage in hypertensive rats. *Food Res. Int.*, **129**: 108862.

Wu HC, Chen HM and Shiau CY (2003). Free amino acids and peptides as related to antioxidant properties in protein hydrolysates of mackerel (*Scomber austriasicus*). *Food Res. Int.*, **36**(9/10): 949-957.

Wu J, Huo J, Huang M, Zhao M, Luo X and Sun BG (2017). Structural characterization of a tetrapeptide from sesame flavor-type Baijiu and its preventive effects against AAPH-induced oxidative stress in HepG2 cells. *J. Agric. Food Chem.*, **65**(48): 10495-10504.

Yang JF, Yang CH, Wu CC and Chuang LY (2015). Antioxidant and antimicrobial activities of the extracts from *Sophora flavescens. J. Pharmacogn. Phytochem.*, **3**(6): 26-31.

Yoshikawa T and You F (2024). Oxidative stress and bio-regulation. *Int. J. Mol. Sci.*, **25**(6): 3360.

Zhang K, Han M, Zhao X, Chen X, Wang H, Ni J and Zhang Y (2022). Hypoglycemic and antioxidant properties of extracts and fractions from *Polygoni avicularis* Herba. *Molecules*, **27**(11): 3381.